SARDet-100K: Towards Open-Source Benchmark and ToolKit for Large-Scale SAR Object Detection

Yuxuan Li[1] **Xiang Li**[1,2,†] **Weijie Li**[3] **Qibin Hou**[1,2] **Li Liu**[3]
Ming-Ming Cheng[1,2] **Jian Yang**[1,†]

[1] PCA Lab, VCIP, CS, Nankai University [2]NKIARI, Futian, Shenzhen
[3]Academy of Advanced Technology Research of Hunan
[†] Corresponding Authors
yuxuan.li.17@ucl.ac.uk, {xiang.li.implus,houqb,cmm,csjyang}@nankai.edu.cn

Abstract

Synthetic Aperture Radar (SAR) object detection has gained significant attention recently due to its irreplaceable all-weather imaging capabilities. However, this research field suffers from both limited public datasets (mostly comprising <2K images with only mono-category objects) and inaccessible source code. To tackle these challenges, we establish a new benchmark dataset and an open-source method for large-scale SAR object detection. Our dataset, SARDet-100K, is a result of intense surveying, collecting, and standardizing 10 existing SAR detection datasets, providing a large-scale and diverse dataset for research purposes. To the best of our knowledge, SARDet-100K is the first COCO-level large-scale multi-class SAR object detection dataset ever created. With this high-quality dataset, we conducted comprehensive experiments and uncovered a crucial challenge in SAR object detection: the substantial disparities between the pretraining on RGB datasets and finetuning on SAR datasets in terms of both data domain and model structure. To bridge these gaps, we propose a novel Multi-Stage with Filter Augmentation (MSFA) pretraining framework that tackles the problems from the perspective of data input, domain transition, and model migration. The proposed MSFA method significantly enhances the performance of SAR object detection models while demonstrating exellent generalizability and flexibility across diverse models. This work aims to pave the way for further advancements in SAR object detection. The dataset and code is available at `https://github.com/zcablii/SARDet_100K`.

1 Introduction

Synthetic Aperture Radar (SAR) [57; 60]is a pivotal technology in remote sensing, providing numerous advantages over traditional optical sensors. Notably, SAR possesses the capability to acquire geographical images under any weather conditions, irrespective of factors such as sunlight, land cover, or certain types of camouflage, as demonstrated in Fig. 1(a). As a consequence of these advantages, SAR has found extensive applications in critical domains, including national defence [48], humanitarian relief [3; 68], camouflage detection [19], and geological exploration [51; 24].

With its invaluable benefits, the field of SAR object detection has garnered increasing attention. In recent years, there has been a substantial increase in the number of research papers focusing on this field, as illustrated in Fig. 1(b). Despite the increasing influence, this research area has suffered from significant challenges including limited resources and transferring gaps.

Limited resources. A significant obstacle in high-resolution SAR image object detection is the sensitivity of SAR images, coupled with the high costs associated with annotating these images. This

38th Conference on Neural Information Processing Systems (NeurIPS 2024).

 https://doi.org/10.52202/079017-4079

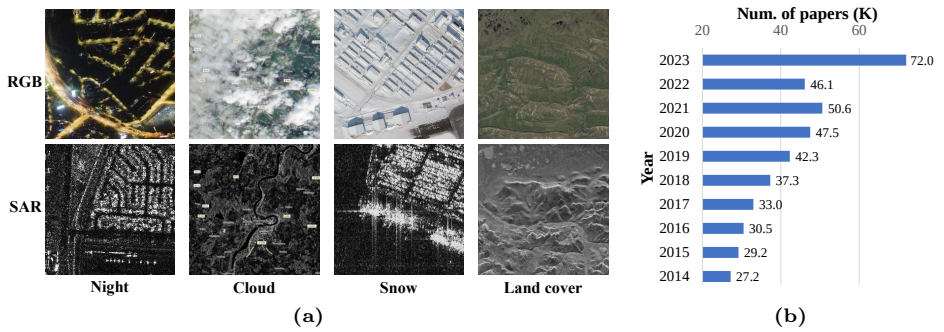

Figure 1: **(a)** Advantages of SAR image: independent of weather conditions, sunlight and land cover. **(b)** Number of papers (thousands) retrieved from Google Scholar using keywords "SAR Detection".

severely restricts the availability of public datasets. Existing datasets, such as SAR-AIRcraft [90], AirSARShip [76], SSDD [84], and HRSID [71], typically consist of a singular type of object against a simplistic background. Moreover, these datasets are generally limited in scale, potentially introducing bias when evaluating different methodologies. Additionally, a notable barrier to advancing research in SAR object detection is the lack of publicly accessible source code, making it challenging to reproduce previous research findings and conduct fair comparisons or build upon existing work.

To address this problem, we merge the most publicly available SAR detection datasets. This effort includes a comprehensive review of current public SAR detection resources, followed by the collection and standardization of these datasets into a uniform format, creating a unified large-scale multi-class dataset for SAR object detection, named SARDet-100k. This dataset comprises approximately 117k images and 246k instances of objects across six distinct categories. To our knowledge, SARDet-100k is the first dataset of COCO-scale magnitude in this research area. It significantly contributes to overcoming the previously mentioned limitations by providing a rich resource for the development and evaluation of SAR object detection models. Moreover, the dataset and source code will be made publicly available.

Transferring gaps. Through our empirical research and detailed analysis, we have identified that a principal hurdle in SAR object detection is the significant domain gap and model gap encountered when transferring a backbone network pretrained on natural RGB datasets (e.g., ImageNet [17]), to a detection network on SAR imagery. The domain gap stems from the stark visual discrepancies between RGB and SAR imagery, whereas the model gap arises from the model differences between the pretrained backbone and the whole detection framework employed in the downstream task.

To mitigate the aforementioned domain gap and model gap, we propose a novel Multi-Stage with Filter Augmentation (MSFA) pretraining framework to bridge these gaps. This framework addresses the challenge from multiple angles: data input, domain transition, and model migration, each tailored to the unique properties of the SAR image detection task. For data input: to address the input domain gap between the pretrain and finetune datasets, we employ traditional, handcrafted feature descriptors. These descriptors efficiently transform the input data from pixel space to a feature space that is not only robust to noise but also statistically narrows the gap between data from RGB and SAR modalities (see Fig. 2(a)), thereby enhancing the transferability of pretrained knowledge. For domain transition: we propose a domain transition bridge utilizing an optical remote sensing detection dataset. This bridge connects natural RGB images through optics correlation and SAR images through object correlation, establishing a hierarchical pretraining approach that effectively closes the domain gap between RGB and SAR imagery (see Fig. 2(b)). For model migration: to guarantee thorough training of the entire detection framework and to facilitate complete model migration for finetuning, we employ the entire detector as a bridging model throughout the multi-stage pretraining process.

The MSFA framework demonstrates remarkable efficacy in reducing the substantial domain and model gaps typically encountered between the pretraining and finetuning stages. MSFA is not only effective but also general and applicable across various modern deep neural networks.

Our contribution to the field of SAR object detection can be concluded into the following FOUR points:

- Introduction of the first COCO-level large-scale dataset for SAR multi-category object detection.
- Identification of critical gaps in traditional model pretrain and finetune approaches for SAR object detection.
- Proposal of a Multi-Stage with Filter Augmentation (MSFA) pretraining framework, which demonstrates remarkable effectiveness, as well as excellent generalizability and flexibility across various deep network models.
- Establishment of a new benchmark in SAR object detection by releasing the datasets and code associated with our research. This contribution is expected to foster further advancements and progress in the field.

2 Related Work

2.1 SAR Images and Handcraft Features

SAR imaging often suffers from poor image quality due to multiplicative speckle noise and artifacts [57; 47]. To mitigate this, many traditional handcrafted feature descriptors have been developed or adapted to extract more discernible features from SAR images. These include Histogram of Oriented Gradients [15] (HOG), Canny Edge Detector [5], Gradient by Ratio Edge (GRE) [29], Haar-like [62] Feature Descriptor and Wavelet Scattering Transform [45] (WST). Early works employed traditional algorithms, such as HOG for SAR object recognition [56; 49], Canny [28; 38] for edge detection. However, in recent years, the field of SAR image analysis has been largely dominated by deep learning approaches.

While recent studies have focused on tasks related to low-level processing [69; 86], classification [83; 85; 93; 26; 50; 78] and pretrain [29; 29], they have attempted to integrate classic handcrafted features into modern neural networks for robust SAR image feature extraction and refinement. In contrast, our work does not simply inject such handcrafted features into networks, but explores the benefits and potentials of handcrafted features in domain adaptation and SAR object detection under modern deep neural networks. This research area remains largely unexplored, and our work aims to bridge this gap.

2.2 SAR Object Detection

Various popular deep learning-based object detection frameworks, including RetinaNet [33], FCOS [59], GFL [30], RCNN series [53; 4], YOLO series [52; 10], and DETR [6], demonstrate remarkable generalizability in the field of general object detection. Additionally, modern backbone networks such as ConvNext [42], VAN [22], LSKNet [31] and Swin Transformer [41] are designed to efficiently and effectively model visual features. However, SAR image object detection poses unique challenges due to factors such as small object size, speckle noise, and sparse information inherent in SAR images. As a result, recent deep learning methods for SAR object detection primarily focus on network and module design to address these challenges. Approaches like MGCAN [9], MSSDNet [91], and SEFEPNet [79] enhance object features through multiscale feature fusion. Quad-FPN [82] combines four distinct feature pyramid networks for thorough multiscale feature interaction to alleviate noise interferences and multi-scale object feature misalignment. PADN [88] and EWFAN [65] employ attention mechanisms to enhance object features in the presence of SAR speckle noise. CenterNet++ [21], an extension of CenterNet [92], incorporates feature enhancement, multi-scale fusion, and head refinement modules to improve the detector's robustness specifically for SAR images. Additionally, CRTransSar [74], built on the high-performance Swin transformer [41], leverages context representation learning to enhance object features.

While most existing works concentrate on mitigating SAR speckle noise interference through network structure improvements, few attempts to address the issue at the level of input data. Furthermore, most studies utilize ImageNet pretrained backbones as the initialization of the detection framework, overlooking the substantial domain gap between the pretrained nature scenes dataset and the finetuned SAR dataset, as well as the model gap between the backbone and the entire detection framework. Instead, we seek to address these unique challenges through a carefully designed pretraining strategy.

 https://doi.org/10.52202/079017-4079

Table 1: Image and instance level statistics of SARDet-100K dataset. *: Origin datasets are cropped into 512 $\times$ 512 patches. Ins: Instances, Img: Images.

Dataset	Images				Instances				Ins/Img
	Train	Val	Test	ALL	Train	Val	Test	ALL	
AIR_SARShip 1* [76]	438	23	40	501	816	33	209	1,058	2.11
AIR_SARShip 2 [76]	270	15	15	300	1,819	127	94	2,040	6.80
HRSID [71]	3,642	981	981	5,604	11,047	2,975	2,947	16,969	3.03
MSAR* [75]	27,159	1,479	1,520	30,158	58,988	3,091	3,123	65,202	2.16
SADD [80]	795	44	44	883	6,891	448	496	7,835	8.87
SAR-AIRcraft* [90]	13,976	1,923	2,989	18,888	27,848	4,631	5,996	38,475	2.04
ShipDataset [67]	31,784	3,973	3,972	39,729	40,761	5,080	5,044	50,885	1.28
SSDD [84]	928	116	116	1,160	2,041	252	294	2,587	2.23
OGSOD [63]	14,664	1,834	1,833	18,331	38,975	4,844	4,770	48,589	2.65
SIVED [35]	837	104	103	1,044	9,561	1,222	1,230	12,013	11.51
SARDet-100k	94,493	10,492	11,613	116,598	198,747	22,703	24,023	245,653	2.11

Table 2: SARDet-100K source datasets information. GF-3: Gaofen-3, S-1: Sentinel-1. Target categories S: ship, A: aircraft, C: car, B: bridge, H: harbour, T: tank.

Datasets	Target	Res. (m)	Band	Polarization	Satellites	License
AIR_SARShip [76]	S	1,3m	C	VV	GF-3	-
HRSID [71]	S	0.5$\sim$3m	C/X	HH, HV, VH, VV	S-1B,TerraSAR-X,TanDEMX	GNU General Public
MSAR [75]	A, T, B, S	$\leq$ 1m	C	HH, HV, VH, VV	HISEA-1	CC BY-NC 4.0
SADD [80]	A	0.5$\sim$3m	X	HH	TerraSAR-X	-
SAR-AIRcraft [90]	A	1m	C	Uni-polar	GF-3	CC BY-NC 4.0
ShipDataset [67]	S	3$\sim$25m	C	HH, VV, VH, HV	S-1,GF-3	-
SSDD [84]	S	1$\sim$15m	C/X	HH, VV, VH, HV	S-1,RadarSat-2,TerraSAR-X	Apache2.0
OGSOD [63]	B, H, T	3m	C	VV/VH	GF-3	-
SIVED [35]	C	0.1,0.3m	Ka,Ku,X	VV/HH	Airborne SAR synthetic slice	-

3 A New Benchmark Dataset for SAR Object Detection

3.1 Current Status

SAR images are typically captured by satellites, and there is a wealth of low-resolution SAR imagery available, often with a Ground Sample Distance (GSD) of 10m $\times$ 10m or larger. Platforms like Sentinel-1 [12] provide access to these images, which offer a macroscopic view of various geophysical places such as cities, mountains, rivers, and cultivated land. This makes them particularly advantageous for scene classification tasks. However, the inherent low resolution of these images constrains their capability to delineate fine details of smaller objects, such as ships, cars, and airplanes. Conversely, high-resolution SAR images provide more detailed information but require significant hardware resources. Moreover, these high-definition images often encompass sensitive information, making them unsuitable for public release. Furthermore, acquiring high-resolution SAR datasets can be very expensive, posing significant challenges to their accessibility.

Numerous research teams frequently encounter budgetary limitations that restrict their capacity to obtain a large and diverse collection of high-resolution SAR datasets. These financial constraints not only limit the scope of geographical areas that can be covered but also affect the variety of data sources that can be accessed. Consequently, the datasets made available by these groups often lack diversity, particularly in aspects such as spectral bands, polarization, and resolution. From a researcher's perspective, evaluating models on such small and homogeneous datasets can introduce bias and lead to unfair performance comparisons.

3.2 SARDet-100K

To address the aforementioned challenges, we undertake a thorough survey of SAR object detection datasets. As a result, we carefully collect a total of **10** publicly available high-quality datasets that are not only diverse but also have no conflicting object categories. These data are released by or collected from different countries and institutions, such as scientific research departments in China, space departments in Europe, and military departments in the United States. Detailed information

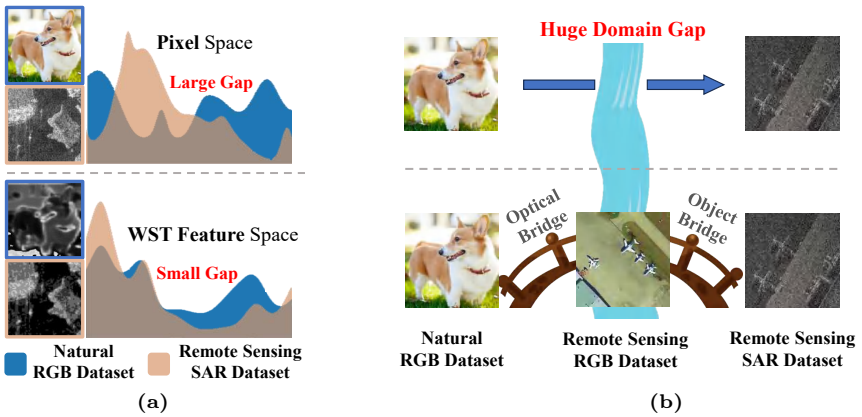

Figure 2: Illustration of the significant domain gap exists between Nature RGB dataset and remote sensing SAR datasets. **(a)** showcases the WST feature space significantly narrows the domain gap. **(b)** demonstrates that the remote sensing RGB dataset serves as an effective domain transit bridge, facilitating smoother domain transfer.

on the collected datasets is shown in Table. 2. To ensure consistency across the collected datasets, we invest considerable time and effort in rigorous dataset standardization. This involves addressing variations in train-val-test splitting status, image resolutions, and annotation formats. More details about data collection and standardization can be found in the Appendix.

Table 1 presents the standardized sub-datasets of SARDet-100K along with their corresponding statistics, which includes information on both image-level and instance-level statistics. The SARDet-100K dataset encompasses a total of 116,598 images, and 245,653 instances distributed across six categories: Aircraft, Ship, Car, Bridge, Tank, and Harbor. SARDet-100K dataset stands as the first large-scale SAR object detection dataset, comparable in size to the widely used COCO [34] dataset (118K images), which is the standard benchmark for general object detection. The scale and diversity of the SARDet-100K dataset effectively simulate real-world scenarios encountered in the application of SAR object detection models across multiple data sources. SARDet-100K provides researchers with robust training and evaluation for advancing SAR object detection algorithms and techniques, fostering the development of SOTA models in this domain.

4 Multi-Stage with Filter Augmentation Pretraining Framework

Several recent studies [26; 78; 74; 21] have demonstrated the effectiveness of mature handcrafted features and specialized network module designs in improving SAR object detection performance. However, most of these works rely on the default ImageNet pretraining approach, thus overlooking the significant domain gap between the pretrained nature scenes dataset and the finetuned SAR dataset. Additionally, they fail to address the model gap that exists between the backbone and the entire detection framework. To address these limitations, we propose a novel framework called the Multi-Stage with Filter Augmentation (MSFA) Pretraining Framework. Our framework tackles the challenges from the perspective of data input, domain transition, and model migration. MSFA comprises two core designs: the Filter Augmented Input and the Multi-Stage pretrain strategy.

4.1 Filter Augmented Input

As discussed in the *Related Work* section, numerous existing handcrafted feature descriptors leverage meticulously designed filters to extract features. These features, robust and rich in information, act as augmented information derived from the original image. Thus, we propose employing such features as auxiliary information alongside the original pixel data. The filter augmented feature M of data x can be generally defined as:

https://doi.org/10.52202/079017-4079

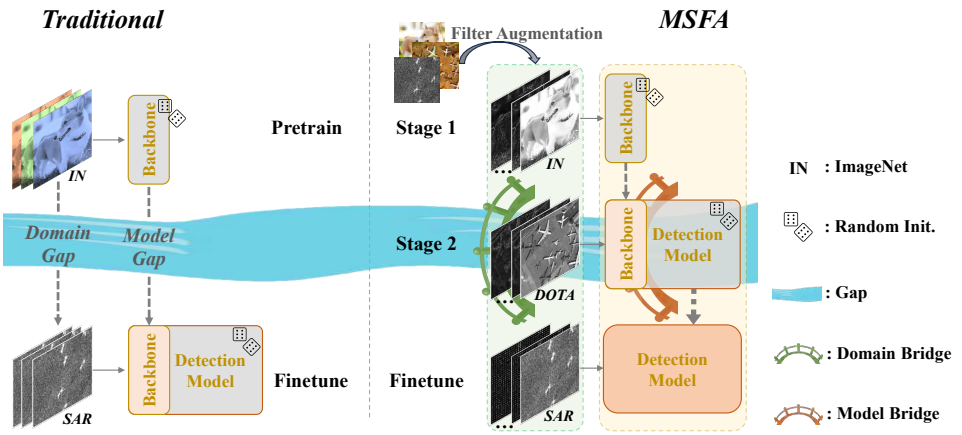

Figure 3: Conceptual illustration of traditional ImageNet pretrain and our proposed Multi-Stage with Filter Augmentation (MSFA) pretrain framework.

$$M_i^x = T_i(x), i \in \{HOG, Canny, Haar, WST, GRE\}. \tag{1}$$

Where T_i is a pre-defined transformation. Drawing inspiration from the information residual design in ResNet [23], we construct the Filter Augmented Input to the detection model, Inp, by concatenating the original grayscale SAR image x with the generated filter augmented feature M_i^x as:

$$Inp = \text{concat}(x, M_i^x). \tag{2}$$

By casting the original data input from the heterogeneous pixel space to a homogeneous filter augmented feature space, the domain gaps between different image domains can be greatly reduced, as illustrated in Fig. 2(a).

4.1.1 Multi-stage pretrain

We formulate the traditional pretrain schema as:

$$B = \text{Train}_{cls}(B_\theta)(D_{IN}), \tag{3}$$

$$A = \text{Train}_{det}(A_B)(D_{SAR}). \tag{4}$$

The function $\text{Train}_t(a)(b)$ means training a model a on a dataset b with a task t, and it returns a trained model. t is the training task, $t \in \{cls, det\}$ where cls stands for classification and det for detection. B indicates the backbone model and A is the whole detection model. Traditionally, the pretrain stage will randomly initialize the backbone model B_θ and train on the dataset ImageNet D_{IN} (as Eq. (3)). Then finetune on the SAR dataset D_{SAR} with pretrained backbone initialised from detection model A_B (as Eq. (4)).

Our proposed multi-stage pretrain strategy, alternatively, can be illustrated as in the Eq. (3) (5) (6).

$$A' = \text{Train}_{det}(A_B)(D_{RS}). \tag{5}$$

$$A = \text{Train}_{det}(A_{A'})(D_{SAR}). \tag{6}$$

Where an extra second stage pretraining in Eq. (5) is added. We propose the utilization of a large-scale optical remote sensing dataset, D_{RS}, as a detection pretrain for domain transit. The dataset consists of optical modal imagery, which also shares similar object shapes, scales, and categories in downstream SAR datasets. This characteristic serves as a valuable bridge between the optical distribution of natural images in ImageNet and the object distribution in SAR remote sensing images. By leveraging such second stage pretrain, the domain gap is effectively minimized, as illustrated in Fig. 2(b).

4.1.2 MSFA

Finally, the proposed MSFA framework integrates Filter Augmented Input with Multi-Stage pretraining, as illustrated in Fig. 3. Our MSFA framework effectively bridges the substantial domain and modal gaps between pretraining on nature images and finetuning on SAR image detection.

By introducing Filter Augmented Input, we leverage mature handcrafted feature descriptors to extract noise-robust features. This also enables us to effectively transform the heterogeneous image domains of both pretraining and finetuning images into a homogeneous feature domain. By unifying the input data into a consistent feature domain, we address the disparities that exist between different types of images. Consequently, it enhances the alignment and transferability of knowledge across domains. Moreover, the incorporation of multi-stage training involves utilizing an additional large-scale optical remote sensing dataset for detection pretraining. This dataset acts as a domain bridge, connecting the domain of ImageNet's nature images with that of SAR remote sensing images. As a result, it further reduces the domain gaps, facilitating a smoother transition between the two domains. Furthermore, the detection pretraining in the second stage of the MSFA framework can also act as a model bridge. It allows for the comprehensive training of the entire detection framework, rather than solely focusing on the backbone, making the whole detection framework well-initialized to perform optimally in the SAR detection finetuning.

5 Experiments and Analysis

5.1 Filter Augmented Input

To investigate and assess the impact of the proposed Filter Augmented Input, we conduct experiments on each traditional feature descriptor discussed in the *Related Work*, within the framework of our proposed MSFA method. The findings, detailed in Table 3, indicate that incorporating these handcrafted features notably enhances the performance of the detector. Additionally, our analysis reveals that converting image pixels into handcrafted feature spaces significantly minimizes the distributional gaps between the ImageNet and the SARDet-100K datasets. This is particularly evident in the Pearson Correlation Coefficients (PCC) between the inputs of the ImageNet and SARDet-100K datasets, as illustrated in Table 4. This underscores the efficacy of the proposed approach in bridging the domain gap between natural and SAR images, thereby enhancing the efficiency of knowledge transfer from the pretraining process.

Input	**mAP** ↑	mAP_{50} ↑
SAR (as RGB)	50.2	83.0
SAR+Canny	50.7	83.6
SAR+Hog	50.7	83.5
SAR+Haar	50.6	83.4
SAR+WST	**51.1**	<u>83.9</u>
SAR+GRE	50.6	83.8
SAR+Hog+Haar+WST	**51.1**	**84.0**

Table 3: Comparison of different Filter Augmented Inputs using Faster R-CNN and ResNet50 as the detection model.

Domain	PCC ↑
Pixel Space	0.394
Canny Space	0.992
Hog Space	0.995
Haar Space	0.990
WST Space	**0.996**
GRE Space	0.984

Table 4: Pearson Correlation Coefficients (PCC) of ImageNet and SARDet-100k on RGB and handcrafted feature spaces.

Remarkably, the Wavelet Scattering Transform (WST) feature stands out for its exceptional performance. This superiority can be attributed not just to its role in significantly narrowing the domain gap, but also to its capacity for extracting rich, multi-scale information. Such information acts as a robust auxiliary feature by mitigating noise and preserving object-related details. However, we also find that using multiple filter augmented features will not have further significant performance gain. It is possible that the existing WST already captures the essential information necessary for effective object detection, and incorporating additional ones does not provide substantial additional beneficial information.

Due to the outstanding performance of WST, we employed it as the default Filter Augmented Input in our MSFA method for the remainder of the paper.

https://doi.org/10.52202/079017-4079

Table 5: Comparison of different pretrain strategies using Faster-RCNN and ResNet50 as the detection model.

ID	Model Input	Pretrain			mAP ↑
		Multi-stage	Dataset	Component	
1	SAR (Raw Pixels)	✗	ImageNet	Backbone	49.0
2		✓	ImageNet + DIOR	Framework	49.5
3		✓	ImageNet + DOTA	Backbone	49.3
4				Framework	**50.2**
5	SAR+WST (Filter Augmented)	✗	ImageNet	Backbone	49.2
6		✓	ImageNet + DIOR	Framework	50.1
7		✓	ImageNet + DOTA	Backbone	49.6
8				Framework	**51.1**

5.2 Multi-stage Pretrain

To evaluate the effectiveness of the proposed multi-stage pretraining approach, we conduct experiments in which we keep the input modality consistent and finetuned the detection model using various pretraining strategies on the SARDet-100K dataset. As a baseline, Exp. 1 takes single-channel SAR data as input, pretrains the backbone model on ImageNet for 100 epochs, and then directly finetune the detector on the SARDet-100K dataset (following the widely used default setting). In addition to the baseline, we perform a second stage pretrain specifically for object detection on optical remote sensing datasets, such as DOTA [73] or DIOR [27]. (Details on DOTA and DIOR datasets can be found in the Appendix). Following the second pretraining stage, we finetune the model either solely on the backbone or on the entire framework.

The results of Exp. 2, 4, 6, and 8 in Table 5 prove the substantial advantages of the two-stage pretraining approach. Notably, even the relatively small-scale DIOR dataset showcases noticeable performance gains compared to the baseline (Exp. 1 and 5). This observation underscores the significance of reducing the domain gap during the pretraining phase of SAR detection.

However, the DIOR dataset pretraining is not as effective as the larger-scale DOTA dataset (Exp. 2 vs 4, 6 vs 8). This comparison underscores the significance of the pretraining scale in achieving optimal results. The DOTA dataset, with its larger scale and similar average instance area to SARDet-100K, provides a more comprehensive and informative pretraining, leading to improved performance during the subsequent finetuning stage.

The comparison between Exp. 3 & 4 and Exp. 7 & 8, demonstrate the superiority of pretraining the entire framework over solely the backbone, highlighting the significant impact of the model gap on the performance of SAR detection.

In summary, our proposed multi-stage pretraining strategy in MSFA alleviates both the data domain gap and the model gap between pretraining and the downstream model, leading to significant enhancements in SAR detection performance. Detailed experimental results and visualization are available in the Appendix.

5.3 Generalizability of MSFA

To assess the effectiveness and generalizability of the proposed MSFA, we conduct experiments using various detectors and backbones, as presented in Fig. 4(a) and 4(b). Significant performance improvement is observed across different frameworks (including single-stage [53; 4; 43], two-stage [33; 30; 59], and end2end [94; 58; 39]) and diverse backbones (including ResNets [23], ConvNexts [42], VANs [22], and Swin-Transformer [41] networks). It provides strong evidence for the effectiveness and wide applicability of our proposed method. Furthermore, we observe stable performance improvements as we scale up the backbone size, as shown in Fig. 4(b), indicating the good scalability of our proposed method.

Significantly, the design of our MSFA method was developed with flexibility, generalizability and wide applicability in mind. Therefore the method can be seamlessly integrated into most existing models without any modifications.

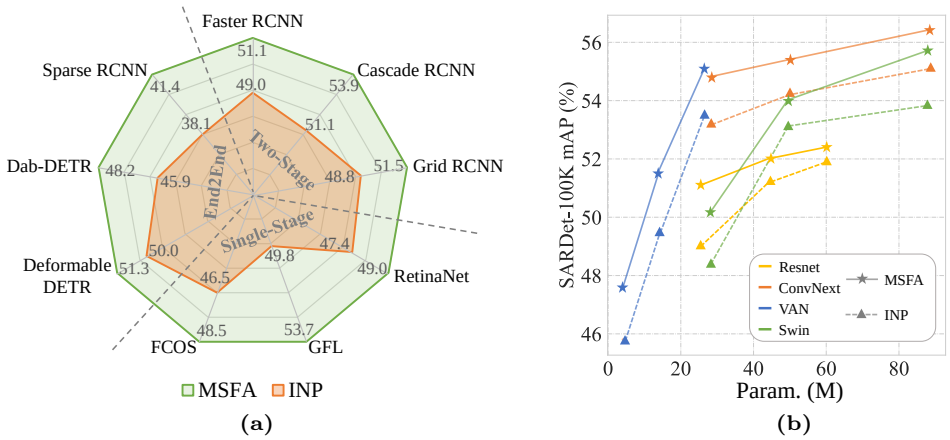

Figure 4: Generalization of MSFA on different detection frameworks **(a)** and different backbones **(b)**. Models are finetuned and tested on SARDet-100K dataset. INP: Traditional ImageNet Pretrain on backbone network only.

Table 6: Comparison of the proposed MSFA with previous state-of-the-art methods on SSDD and HRSID datasets.

Detectors		Open Source	Year	mAP_{50} ↑	
				SSDD	HRSID
General Detectors	Grid R-CNN [43]	✓	2019	88.9	79.4
	Faster R-CNN [53]	✓	2015	89.7	80.7
	Cascade R-CNN [4]	✓	2019	90.5	81.3
	Free-Anchor [87]	✓	2019	91.0	81.8
	Double-Head R-CNN [72]	✓	2020	91.1	82.1
	PANET [40]	✓	2018	91.2	81.6
	DCN [14]	✓	2017	92.3	82.1
SAR Detectors	NNAM [7]	✗	2019	79.8	-
	DCMSNM [25]	✗	2018	89.6	-
	ARPN [89]	✗	2020	89.9	81.8
	DAPN [13]	✗	2019	90.6	81.8
	HR-SDNet [70]	✗	2020	90.8	82.5
	SER Faster R-CNN [37]	✗	2018	91.5	81.5
	FBR-Net [20]	✗	2020	94.1	-
	NRENet [44]	✗	2024	94.6	75.6
	CenterNet++ [21]	✗	2021	95.1	-
	CRTransSar [74]	✗	2022	97.0	-
	SARATR-X [77]	✗	2024	97.3	80.3
Faster R-CNN + VAN-B		✓	2023	92.9	81.8
MSFA (Faster R-CNN + VAN-B)		✓	2024	**97.9**(+5.0)	**83.7**(+1.9)

5.4 Comparison with SOTAs

We compare various SOTA methods, including both general object detection models [43; 53; 14; 64; 4; 87; 72], as well as SAR object detection models [7; 25; 89; 13; 70; 40; 37; 74; 21; 20]. We evaluate their performance on the SSDD and HRSID datasets, which are the commonly used benchmarks for SAR object detection. To leverage the superior efficiency and performance of the VAN [22] backbone (as shown in Fig. 4(b)), we employ the classic faster R-CNN detection framework with the lightweight VAN-B (Param. 26.6M) backbone as our detection model. The results presented in Table 6 demonstrate that our MSFA method outperforms all the compared methods by a significant margin. Specifically, MSFA achieves a mAP@50 of 97.9% on the SSDD dataset and a mAP@50 of 83.7% on the HRSID dataset, setting new state-of-the-art results. It is noteworthy that our method is the only open-sourced method among the compared SAR detection SOTAs.

https://doi.org/10.52202/079017-4079

6 Limitaion and Future Work

The scope of this paper is limited to supervised pretraining. However, considering the availability of a vast amount of unannotated SAR images, it would be valuable to explore the potential of semi-supervised, weakly-supervised or unsupervised learning methods for domain transfer in SAR object detection.

While this paper aims to propose a simple, practical, effective, and generic method, it does not delve into the details of specific designs. Future work can be expanded to explore the aforementioned directions in more depth, incorporating intricate and specialized designs to enhance the performance and capabilities of SAR object detection.

7 Conclusion

This paper presents a new benchmark for large-scale SAR object detection, introducing the SARDet-100k dataset and the Multi-Stage with Filter Augmentation (MSFA) pretrain method. Our SARDet-100k dataset comprises over 116K images spanning 6 categories, providing a large and diverse dataset for conducting SAR object detection research. To bridge the domain and model gaps between pretraining and finetuning stages in SAR object detection, we propose the MSFA pretraining framework. MSFA significantly enhances the performance of SAR object detection models, setting new state-of-the-art performance in previous benchmark datasets. Moreover, MSFA demonstrates remarkable generalizability and flexibility across various models. Our research endeavours to overcome the current obstacles prevalent in SAR object detection. We anticipate our contributions will pave the way for future research and innovations in this domain.

Our research endeavours to overcome the current obstacles prevalent in SAR object detection. We anticipate our contributions will pave the way for future research and innovations in this domain.

8 Acknowledgement

We extend our deepest gratitude to the following researchers, listed alphabetically by first name: Hong Zhang, Runfan Xia, Shunjun Wei, Tianwen Zhang, Xian Sun, Xiaofang Zhu, Xiaoling Zhang, and other contributing researchers, for allowing us to integrate their datasets. Their contributions have greatly advanced and promoted research in this field.

This work is supported by the National Science Fund of China (62361166670,62276145, 62176130, 62206134) and the Fundamental Research Funds for the Central Universities (Nankai University: 070-63233084, 070-63243142). Computation is supported by the Supercomputing Center of Nankai University (NKSC).

References

[1] Ai, J., Tian, R., Luo, Q., Jin, J., Tang, B.: Multi-scale rotation-invariant haar-like feature integrated cnn-based ship detection algorithm of multiple-target environment in sar imagery. TGRS (2019)

[2] Besnassi, M., Neggaz, N., Benyettou, A.: Face detection based on evolutionary haar filter. Pattern Analysis and Applications (2020)

[3] Braun, A.: Radar satellite imagery for humanitarian response. Bridging the gap between technology and application. Ph.D. thesis, Universität Tübingen (2019)

[4] Cai, Z., Vasconcelos, N.: Cascade R-CNN: High quality object detection and instance segmentation. TPAMI (2019)

[5] Canny, J.: A computational approach to edge detection. TPAMI (1986)

[6] Carion, N., Massa, F., Synnaeve, G., Usunier, N., Kirillov, A., Zagoruyko, S.: End-to-end object detection with transformers. In: ECCV (2020)

[7] Chen, C., He, C., Hu, C., Pei, H., Jiao, L.: A deep neural network based on an attention mechanism for sar ship detection in multiscale and complex scenarios. IEEE Access (2019)

[8] Chen, K., Wang, J., Pang, J., Cao, Y., Xiong, Y., Li, X., Sun, S., Feng, W., Liu, Z., Xu, J., et al.: Mmdetection: Open mmlab detection toolbox and benchmark. arXiv (2019)

[9] Chen, L., Luo, R., Xing, J., Li, Z., Yuan, Z., Cai, X.: Geospatial transformer is what you need for aircraft detection in sar imagery. TGRS (2022)

[10] Chen, Y., Yuan, X., Wu, R., Wang, J., Hou, Q., Cheng, M.M.: YOLO-MS: Rethinking multi-scale representation learning for real-time object detection. arXiv (2023)

[11] Contributors, M.: Openmmlab's pre-training toolbox and benchmark. `https://github.com/openmmlab/mmpretrain` (2024)

[12] Contributors, S..: Sentinel-1 - missions. `https://sentinels.copernicus.eu/web/sentinel/missions/sentinel-1` (2024)

[13] Cui, Z., Li, Q., Cao, Z., Liu, N.: Dense attention pyramid networks for multi-scale ship detection in sar images. TGRS (2019)

[14] Dai, J., Qi, H., Xiong, Y., Li, Y., Zhang, G., Hu, H., Wei, Y.: Deformable convolutional networks. In: ICCV. pp. 764–773 (2017)

[15] Dalal, N., Triggs, B.: Histograms of oriented gradients for human detection. In: CVPR (2005)

[16] Dellinger, F., Delon, J., Gousseau, Y., Michel, J., Tupin, F.: SAR-SIFT: a SIFT-like algorithm for SAR images. TGRS (2014)

[17] Deng, J., Dong, W., Socher, R., Li, L.J., Li, K., Fei-Fei, L.: ImageNet: A large-scale hierarchical image database. In: CVPR (2009)

[18] Feng, Y., Han, B., Wang, X., Shen, J., Guan, X., Ding, H.: Self-supervised transformers for unsupervised sar complex interference detection using canny edge detector. Remote Sensing (2024)

[19] Frolind, P.O., Gustavsson, A., Lundberg, M., Ulander, L.M.: Circular-aperture vhf-band synthetic aperture radar for detection of vehicles in forest concealment. IEEE Transactions on Geoscience and Remote Sensing (2011)

[20] Fu, J., Sun, X., Wang, Z., Fu, K.: An anchor-free method based on feature balancing and refinement network for multiscale ship detection in sar images. TGRS (2020)

[21] Guo, H., Yang, X., Wang, N., Gao, X.: A centernet++ model for ship detection in sar images. Pattern Recognition (2021)

[22] Guo, M.H., Lu, C., Liu, Z.N., Cheng, M.M., Hu, S.: Visual attention network. Computational Visual Media (2022)

[23] He, K., Zhang, X., Ren, S., Sun, J.: Deep residual learning for image recognition. In: Proceedings of the IEEE conference on computer vision and pattern recognition. pp. 770–778 (2016)

[24] Ivanov, A.Y., Gerivani, H., Evtushenko, N.V.: Characterization of natural hydrocarbon seepage in the south caspian sea off iran using satellite sar and geological data. Marine Georesources & Geotechnology (2020)

[25] Jiao, J., Zhang, Y., Sun, H., Yang, X., Gao, X., Hong, W., Fu, K., Sun, X.: A densely connected end-to-end neural network for multiscale and multiscene sar ship detection. IEEE Access (2018)

[26] Jin, Y., Duan, Y.: Wavelet scattering network-based machine learning for ground penetrating radar imaging: Application in pipeline identification. Remote Sensing (2020)

[27] Li, K., Wan, G., Cheng, G., Meng, L., Han, J.: Object detection in optical remote sensing images: A survey and a new benchmark. ISPRS (2020)

 https://doi.org/10.52202/079017-4079

[28] Li, W., He, M., Zhang, S.: A new canny-based edge detector for sar image. In: Congress on Image and Signal Processing (2008)

[29] Li, W., Wei, Y., Liu, T., Hou, Y., Liu, Y., Liu, L.: Self-supervised learning for sar atr with a knowledge-guided predictive architecture. arXiv (2023)

[30] Li, X., Lv, C., Wang, W., Li, G., Yang, L., Yang, J.: Generalized focal loss: Towards efficient representation learning for dense object detection. TPAMI (2022)

[31] Li, Y., Hou, Q., Zheng, Z., Cheng, M.M., Yang, J., Li, X.: Large selective kernel network for remote sensing object detection. In: ICCV (2023)

[32] Lienhart, R., Maydt, J.: An extended set of haar-like features for rapid object detection. In: International Conference on Image Processing (2002)

[33] Lin, T.Y., Goyal, P., Girshick, R., He, K., Dollár, P.: Focal loss for dense object detection. In: ICCV (2017)

[34] Lin, T.Y., Maire, M., Belongie, S.J., Hays, J., Perona, P., Ramanan, D., Dollár, P., Zitnick, C.L.: Microsoft COCO: Common objects in context. In: ECCV (2014)

[35] Lin, X., Zhang, B., Wu, F., Wang, C., Yang, Y., Chen, H.: Sived: A sar image dataset for vehicle detection based on rotatable bounding box. Remote Sensing (2023)

[36] Lin, Y.N., Hsieh, T.Y., Huang, J.J., Yang, C.Y., Shen, V.R., Bui, H.H.: Fast iris localization using haar-like features and adaboost algorithm. Multimedia Tools and Applications (2020)

[37] Lin, Z., Ji, K., Leng, X., Kuang, G.: Squeeze and excitation rank faster r-cnn for ship detection in sar images. IEEE Geoscience and Remote Sensing Letters (2018)

[38] Liu, H., Jezek, K.: Automated extraction of coastline from satellite imagery by integrating canny edge detection and locally adaptive thresholding methods. International journal of remote sensing (2004)

[39] Liu, S., Li, F., Zhang, H., Yang, X., Qi, X., Su, H., Zhu, J., Zhang, L.: DAB-DETR: Dynamic anchor boxes are better queries for DETR. In: ICLR (2022)

[40] Liu, S., Qi, L., Qin, H., Shi, J., Jia, J.: Path aggregation network for instance segmentation. In: CVPR (2018)

[41] Liu, Z., Lin, Y., Cao, Y., Hu, H., Wei, Y., Zhang, Z., Lin, S., Guo, B.: Swin transformer: Hierarchical vision transformer using shifted windows. In: CVPR (2021)

[42] Liu, Z., Mao, H., Wu, C.Y., Feichtenhofer, C., Darrell, T., Xie, S.: A convnet for the 2020s. In: CVPR (2022)

[43] Lu, X., Li, B., Yue, Y., Li, Q., Yan, J.: Grid r-cnn. In: CVPR. pp. 7363–7372 (2019)

[44] Ma, W., Yang, X., Zhu, H., Wang, X., Yi, X., Wu, Y., Hou, B., Jiao, L.: Nrenet: Neighborhood removal-and-emphasis network for ship detection in sar images. International Journal of Applied Earth Observation and Geoinformation (2024)

[45] Mallat, S.: Group invariant scattering. Communications on Pure and Applied Mathematics (2012)

[46] Mita, T., Kaneko, T., Hori, O.: Joint haar-like features for face detection. In: ICCV (2005)

[47] Moreira, A., Prats-Iraola, P., Younis, M., Krieger, G., Hajnsek, I., Papathanassiou, K.P.: A tutorial on synthetic aperture radar. IEEE Geoscience and remote sensing magazine (2013)

[48] Peng, B., Peng, B., Zhou, J., Xie, J., Liu, L.: Scattering model guided adversarial examples for sar target recognition: Attack and defense. IEEE Transactions on Geoscience and Remote Sensing (2022)

[49] Qi, S., Ma, J., Lin, J., Li, Y., Tian, J.: Unsupervised ship detection based on saliency and s-hog descriptor from optical satellite images. IEEE geoscience and remote sensing letters (2015)

[50] Qin, R., Fu, X., Chang, J., Lang, P.: Multilevel wavelet-srnet for sar target recognition. IEEE Geoscience and Remote Sensing Letters (2021)

[51] Ramadan, T.M., Onsi, H.M.: Use of ers-2 sar and landsat tm images for geological mapping and mineral exploration of sol hamid area, south eastern desert, egypt. Egyptian Journal of Remote Sensing and Space Sciences (2003)

[52] Redmon, J., Divvala, S., Girshick, R., Farhadi, A.: You only look once: Unified, real-time object detection. In: CVPR (2016)

[53] Ren, S., He, K., Girshick, R., Sun, J.: Faster R-CNN: Towards real-time object detection with region proposal networks. In: NeurIPS (2015)

[54] Schwegmann, C.P., Kleynhans, W., Salmon, B.P.: Ship detection in south african oceans using sar, cfar and a haar-like feature classifier. In: IEEE Geoscience and Remote Sensing Symposium (2014)

[55] Schwegmann, C.P., Kleynhans, W., Salmon, B.P.: Synthetic aperture radar ship detection using haar-like features. IEEE Geoscience and Remote Sensing Letters (2016)

[56] Song, S., Xu, B., Yang, J.: Sar target recognition via supervised discriminative dictionary learning and sparse representation of the sar-hog feature. Remote Sensing (2016)

[57] Sun, G.C., Liu, Y., Xiang, J., Liu, W., Xing, M., Chen, J.: Spaceborne synthetic aperture radar imaging algorithms: An overview. IEEE Geoscience and Remote Sensing Magazine (2021)

[58] Sun, P., Zhang, R., Jiang, Y., Kong, T., Xu, C., Zhan, W., Tomizuka, M., Li, L., Yuan, Z., Wang, C., et al.: Sparse r-cnn: End-to-end object detection with learnable proposals. In: CVPR (2021)

[59] Tian, Z., Shen, C., Chen, H., He, T.: Fcos: Fully convolutional one-stage object detection. In: ICCV (2019)

[60] Tsokas, A., Rysz, M., Pardalos, P.M., Dipple, K.: Sar data applications in earth observation: An overview. Expert Systems with Applications (2022)

[61] Vidal-Pantaleoni, A., Marti, D.: Comparison of different speckle-reduction techniques in sar images using wavelet transform. International Journal of Remote Sensing (2004)

[62] Viola, P., Jones, M.: Rapid object detection using a boosted cascade of simple features. In: CVPR (2001)

[63] Wang, C., Ruan, R., Zhao, Z., Li, C., Tang, J.: Category-oriented localization distillation for sar object detection and a unified benchmark. IEEE Transactions on Geoscience and Remote Sensing (2023)

[64] Wang, J., Chen, K., Yang, S., Loy, C.C., Lin, D.: Region proposal by guided anchoring. In: CVPR (2019)

[65] Wang, J., Xiao, H., Chen, L., Xing, J., Pan, Z., Luo, R., Cai, X.: Integrating weighted feature fusion and the spatial attention module with convolutional neural networks for automatic aircraft detection from sar images. Remote Sensing (2021)

[66] Wang, Y., Hernández, H.H., Albrecht, C.M., Zhu, X.X.: Feature guided masked autoencoder for self-supervised learning in remote sensing. arXiv (2023)

[67] Wang, Y., Wang, C., Zhang, H., Dong, Y., Wei, S.: A sar dataset of ship detection for deep learning under complex backgrounds. remote sensing **11**(7), 765 (2019)

[68] Wegmuller, U., Wiesmann, A., Strozzi, T., Werner, C.: Envisat asar in disaster management and humanitarian relief. In: IEEE International Geoscience and Remote Sensing Symposium (2002)

[69] Wei, Q.R., Wang, Y.K., Xie, P.Y.: Sar edge detector with high localization accuracy. In: International Geoscience and Remote Sensing Symposium (2019)

 https://doi.org/10.52202/079017-4079

[70] Wei, S., Su, H., Ming, J., Wang, C., Yan, M., Kumar, D., Shi, J., Zhang, X.: Precise and robust ship detection for high-resolution sar imagery based on hr-sdnet. Remote Sensing (2020)

[71] Wei, S., Zeng, X., Qu, Q., Wang, M., Su, H., Shi, J.: Hrsid: A high-resolution sar images dataset for ship detection and instance segmentation. IEEE Access (2020)

[72] Wu, Y., Chen, Y., Yuan, L., Liu, Z., Wang, L., Li, H., Fu, Y.: Rethinking classification and localization for object detection. In: CVPR (2020)

[73] Xia, G.S., Bai, X., Ding, J., Zhu, Z., Belongie, S., Luo, J., Datcu, M., Pelillo, M., Zhang, L.: DOTA: A large-scale dataset for object detection in aerial images. In: CVPR (2018)

[74] Xia, R., Chen, J., Huang, Z., Wan, H., Wu, B., Sun, L., Yao, B., Xiang, H., Xing, M.: Crtranssar: A visual transformer based on contextual joint representation learning for sar ship detection. Remote Sensing (2022)

[75] Xia, R., Chen, J., Huang, Z., Wan, H., Wu, B., Sun, L., Yao, B., Xiang, H., Xing, M.: Crtranssar: A visual transformer based on contextual joint representation learning for sar ship detection. Remote Sensing (2022)

[76] Xian, S., Zhirui, W., Yuanrui, S., Wenhui, D., Yue, Z., Kun, F.: Air-sarship-1.0: High-resolution sar ship detection dataset. J. Radars (2019)

[77] Yang, W., Hou, Y., Liu, L., Liu, Y., Li, X., et al.: Saratr-x: A foundation model for synthetic aperture radar images target recognition. arXiv (2024)

[78] Zhang, J., Xing, M., Xie, Y.: Fec: A feature fusion framework for sar target recognition based on electromagnetic scattering features and deep cnn features. TGRS (2020)

[79] Zhang, P., Xu, H., Tian, T., Gao, P., Li, L., Zhao, T., Zhang, N., Tian, J.: Sefepnet: Scale expansion and feature enhancement pyramid network for sar aircraft detection with small sample dataset. IEEE Journal of Selected Topics in Applied Earth Observations and Remote Sensing (2022)

[80] Zhang, P., Xu, H., Tian, T., Gao, P., Li, L., Zhao, T., Zhang, N., Tian, J.: Sefepnet: Scale expansion and feature enhancement pyramid network for sar aircraft detection with small sample dataset. IEEE Journal of Selected Topics in Applied Earth Observations and Remote Sensing (2022)

[81] Zhang, S., Bauckhage, C., Cremers, A.B.: Informed haar-like features improve pedestrian detection. In: CVPR (2014)

[82] Zhang, T., Zhang, X., Ke, X.: Quad-fpn: A novel quad feature pyramid network for sar ship detection. Remote Sensing (2021)

[83] Zhang, T., Zhang, X., Ke, X., Liu, C., Xu, X., Zhan, X., Wang, C., Ahmad, I., Zhou, Y., Pan, D., et al.: Hog-shipclsnet: A novel deep learning network with hog feature fusion for sar ship classification. TGRS (2021)

[84] Zhang, T., Zhang, X., Li, J., Xu, X., Wang, B., Zhan, X., Xu, Y., Ke, X., Zeng, T., Su, H., et al.: Sar ship detection dataset (ssdd): Official release and comprehensive data analysis. Remote Sensing (2021)

[85] Zhang, T., Zhang, X., Shi, J., Wei, S.: A hog feature fusion method to improve cnn-based sar ship classification accuracy. In: IEEE International Geoscience and Remote Sensing Symposium (2021)

[86] Zhang, W.: Combination of sift and canny edge detection for registration between sar and optical images. IEEE Geoscience and Remote Sensing Letters (2020)

[87] Zhang, X., Wan, F., Liu, C., Ji, R., Ye, Q.: Freeanchor: Learning to match anchors for visual object detection. NeurIPS (2019)

[88] Zhao, Y., Zhao, L., Li, C., Kuang, G.: Pyramid attention dilated network for aircraft detection in sar images. IEEE Geoscience and Remote Sensing Letters (2020)

[89] Zhao, Y., Zhao, L., Xiong, B., Kuang, G.: Attention receptive pyramid network for ship detection in sar images. IEEE Journal of Selected Topics in Applied Earth Observations and Remote Sensing (2020)

[90] Zhirui, W., Yuzhuo, K., Xuan, Z., Yuelei, W., Ting, Z., Xian, S.: Sar-aircraft-1.0: High-resolution sar aircraft detection and recognition dataset. J. Radars (2023)

[91] Zhou, K., Zhang, M., Wang, H., Tan, J.: Ship detection in sar images based on multi-scale feature extraction and adaptive feature fusion. Remote Sensing (2022)

[92] Zhou, X., Wang, D., Krähenbühl, P.: Objects as points. arXiv (2019)

[93] Zhu, H., Wong, T., Lin, N., Lung, H., Li, Z., Thedoridis, S.: A new target classification method for synthetic aperture radar images based on wavelet scattering transform. In: ICSPCC (2020)

[94] Zhu, X., Su, W., Lu, L., Li, B., Wang, X., Dai, J.: Deformable detr: Deformable transformers for end-to-end object detection. arXiv preprint arXiv:2010.04159 (2020)

 https://doi.org/10.52202/079017-4079

A Appendix

A.1 SARDet-100K Dataset Visualization

Fig. S5 offers a visualization of sample images from the proposed SARDet-100K dataset. Representative samples for each category, including Ship, Tank, Bridge, Harbour, Aircraft, and Car, are showcased.

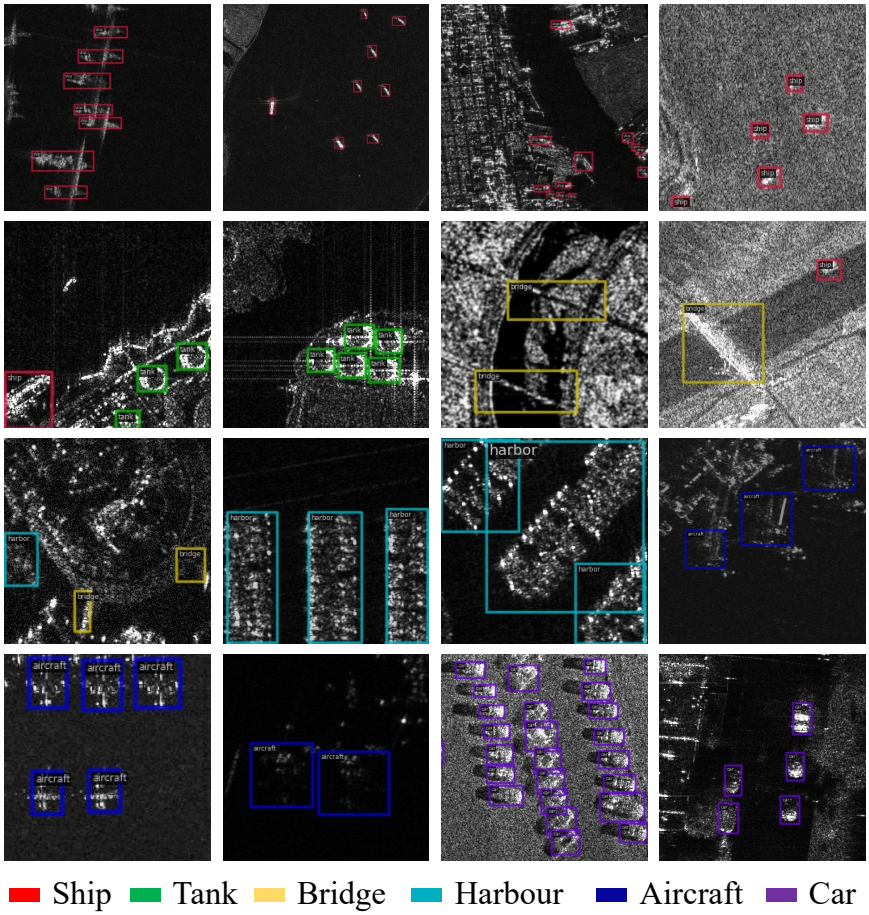

Figure S5: Visualization of sample images from the proposed SARDet-100K dataset.

A.2 Standardization.

We collect a total of **10** publicly available high-quality datasets that are not only diverse but also have no conflicting object categories. These data are released by or collected from different countries and institutions, such as scientific research departments in China, space departments in Europe, and military departments in the United States. To ensure consistency across the collected datasets, it is necessary to undertake standardization processes. This involves addressing variations in train-val-test splitting status, image resolutions, and annotation formats. The overview of SARDet-100K dataset process pipeline is illustrated in Fig. S6(a).

If the source dataset already provides predefined train, validation, and test splits, we adopt their split settings. Otherwise, we perform the splitting by ensuring a ratio of 8:1:1 for the train, validation, and test sets respectively.

Additionally, we tackle the issue of high image resolution in some of the collected datasets. This concern arises because resizing these images before passing them to the model could result in extremely small targets. We perform image slicing on all datasets that contain images larger than

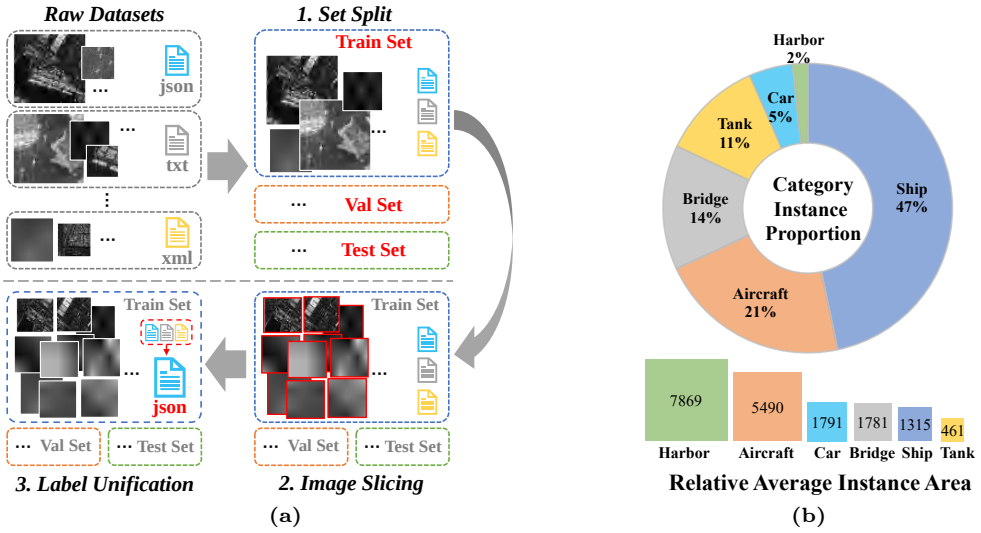

Figure S6: **(a)** SARDet-100K dataset standardization process, encompassing set splitting, large image slicing, and label annotation format unification. **(b)** Percentage of instances for each category and average instance area (in pixels) in SARDet-100K.

1000×1000 resolution. Specifically, for AIR SARShip 1, MSAR, and SAR-AIRcraft datasets, we crop each image into patches of size 512×512 with a patch overlap of 200.

Furthermore, we convert all dataset annotations into the COCO annotation format [34]. This step ensures consistency and compatibility among the different datasets. Consequently, the merged dataset, SARDet-100K, is also standardized in the COCO format, which is readily compatible with popular open-source detection code frameworks, eliminating the need for additional manual data preprocessing. Fig. S6(b) provides an overview of the category-level statistics for the SARDet-100K dataset.

https://doi.org/10.52202/079017-4079

A.3 Handcrafted Feature Descriptors

Histogram of Oriented Gradients [15] (HOG). HOG is a widely used local feature descriptor in image processing and computer vision. It captures and represents the image's local structure and shape information by analyzing the distribution of gradient orientations. HOG is proven to be effective for SAR image classification and object detection tasks because it is invariant to random noise in SAR images. Early works employ HOG for SAR object recognition [56; 49], and recent studies demonstrate the effectiveness of HOG features for SAR image classification [83; 85], as well as the model pretraining [66] in modern neural networks.

Canny Edge Detector [5]. Canny is a widely used edge detection algorithm, which aims to identify significant edges in an image while minimizing noise and spurious responses. The algorithm utilizes Gaussian smoothing, pixel orientation gradient magnitude, and non-maximum suppression. Early research [28; 38] recognize the advantage of Canny for SAR image processing. Recent works also verify the effectiveness of the Canny feature in SAR image edge detection [69], interference detection [18], and image registration [86]. Other than Canny Edge Detector, Gradient by Ratio Edge (GRE) [29], a recently proposed edge detector, leverages SAR-HOG [16] and SAR-SIFT [56] to achieve effective edge detection in SAR images.

Haar-like [62] Feature Descriptor. Haar-like features are commonly used for face detection [46; 2], pedestrian detection [81], and other target detection tasks [32; 36]. They describe the characteristics of an image by utilizing predefined feature templates. Haar-like features can capture linear features, edge features, point features, and diagonal features. Early studies [54; 55] demonstrate the robustness of Haar-like features for SAR object detection. A recent approach called MSRIHL [1] integrates low-level Haar-like features into deep learning models for accurate SAR object detection, highlighting its potential effectiveness.

Wavelet Scattering Transform [45] (WST). The WST is a powerful signal-processing technique that is widely used in image processing. It aims to extract robust and discriminative low-level and high-level features simultaneously. By capturing both high-frequency and low-frequency information, it provides a rich representation of both local and global image features. The hierarchical representation offered by the Wavelet Scattering Transform enables feature extraction at different scales and resolutions, which is particularly useful for capturing fine details of small objects in SAR images and robustly handling high-frequency noise. Vidal et al. [61] conduct a comprehensive investigation demonstrating the high potential performance of Wavelet Transform in SAR image denoising. Many recent works [93; 26; 50; 78] utilize Wavelet Transform or WST for robust feature extraction and integration with CNN networks for target recognition. These studies validate the feasibility of incorporating WST features into modern CNN models.

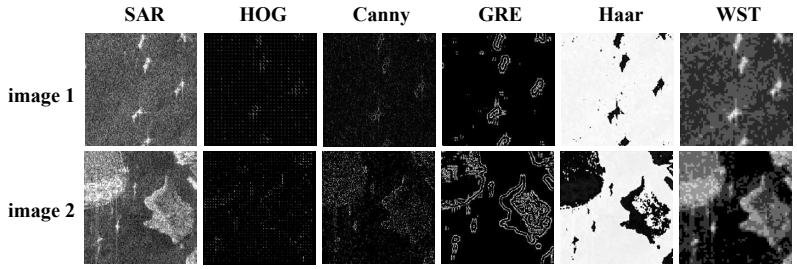

Figure S7: Visualization of handcrafted features on SAR images. (To facilitate visualization, the features are average pooled and represented as a single channel.

A.4 Multi-Stage Filter-Augmentation

Fig. S8 provides a visual illustration of the proposed filter-augmented data input. It involves concatenating the original single-channel grayscale Synthetic Aperture Radar (SAR) image, denoted as x, with the filter-augmentation representation M_i^x.

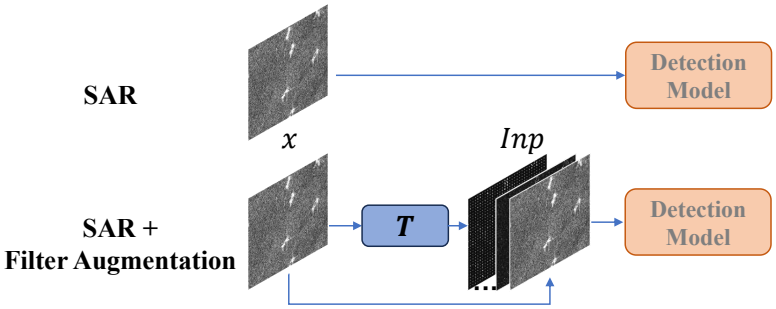

Figure S8: Illustration of filter-augmented input.

Table S7: Comparsion of different filter augmented inputs using Faster R-CNN and Resnet-50 as detection model.

Modality	**mAP**	@50	@75	@s	@m	@l
SAR (as RGB)	50.2	83.0	54.8	44.8	61.6	58.6
SAR+Canny	50.7	83.6	55.0	45.3	62.0	57.1
SAR+Hog	50.7	83.5	55.2	45.1	61.4	**58.4**
SAR+Haar	50.6	83.4	54.7	45.4	61.6	58.0
SAR+WST	**51.1**	83.9	54.7	45.2	**62.3**	57.5
SAR+GRE	50.6	83.8	54.7	44.8	61.7	57.6
SAR+Hog+Haar+WST	**51.1**	**84.0**	**55.9**	**45.7**	62.0	58.2

Table S8: Generalization of MSFA on different detection frameworks. INP: Traditional ImageNet Pretrain on backbone network only.

Framework		Pretrain	Test					
			mAP	@50	@75	@s	@m	@l
Two Stage	Faster RCNN [53]	INP	49.0	82.2	52.9	43.5	60.6	55.0
		MSFA	51.1 (+2.1)	83.9	54.7	45.2	62.3	57.5
	Cascade RCNN [4]	INP	51.1	81.9	55.8	44.9	62.9	60.3
		MSFA	53.9 (+2.8)	83.4	59.8	47.2	66.1	63.2
	Grid RCNN [4]	INP	48.8	79.1	52.9	42.4	61.9	55.5
		MSFA	**51.5** (+2.7)	81.7	56.3	45.1	64.1	60.0
Single Stage	RetinaNet [33]	INP	47.4	79.3	49.7	40.0	59.2	57.5
		MSFA	49.0 (+1.6)	80.1	52.6	41.3	61.1	59.4
	GFL [30]	INP	49.8	80.9	53.3	42.3	62.4	58.1
		MSFA	53.7 (+3.9)	84.2	57.8	47.8	66.2	59.5
	FCOS [59]	INP	46.5	80.9	49.0	41.1	59.2	50.4
		MSFA	48.5 (+2.0)	82.1	51.4	42.9	60.4	56.0
End to End	DETR [6]	INP	31.8	62.3	30.0	22.2	44.9	41.1
		MSFA	47.2 (+15.4)	77.5	49.8	37.9	62.9	58.2
	Deformable DETR [94]	INP	50.0	85.1	51.7	44.0	65.1	61.2
		MSFA	51.3 (+1.3)	85.3	54.0	44.9	65.6	61.7
	Sparse RCNN [58]	INP	38.1	68.8	38.8	29.0	51.3	48.7
		MSFA	41.4 (+3.3)	74.1	41.8	33.6	53.9	53.4
	Dab-DETR [39]	INP	45.9	79.0	47.9	38.0	61.1	55.0
		MSFA	48.2 (+2.3)	81.1	51.0	41.2	63.1	55.4

https://doi.org/10.52202/079017-4079

Table S9: Generalization of MSFA on different detection backbones. INP: Traditional ImageNet Pretrain on backbone network only.

Framework	#P(M)	Pretrain	Test					
			mAP	@50	@75	@s	@m	@l
R50 [23]	25.6	INP	49.0	82.2	52.9	43.5	60.6	55.0
		MSFA	51.1 **(+2.1)**	83.9	54.7	45.2	62.3	57.5
R101 [23]	44.7	INP	51.2	84.1	55.6	45.9	61.9	56.3
		MSFA	52.0 **(+0.8)**	84.6	56.6	46.6	63.4	57.7
R152 [23]	60.2	INP	51.9	85.2	55.9	46.4	62.5	57.9
		MSFA	52.4 **(+0.5)**	85.4	57.2	47.4	63.3	58.7
ConvNext-T [42]	28.6	INP	53.2	86.3	58.1	47.2	65.2	59.6
		MSFA	54.8 **(+1.6)**	87.1	59.8	48.8	66.7	62.1
ConvNext-S [42]	50.1	INP	54.2	87.8	59.2	49.2	65.8	59.8
		MSFA	55.4 **(+1.2)**	87.6	60.7	50.1	67.1	61.3
ConvNext-B [42]	88.6	INP	55.1	87.8	59.5	48.9	66.9	61.1
		MSFA	56.4 **(+1.3)**	88.2	61.5	51.1	68.3	62.4
VAN-T [22]	4.1	INP	45.8	79.8	48.0	38.6	57.9	53.3
		MSFA	47.6 **(+1.8)**	81.4	50.6	40.5	59.4	56.7
VAN-S [22]	13.9	INP	49.5	83.8	52.8	43.2	61.6	56.4
		MSFA	51.5 **(+2.0)**	85.0	55.6	44.8	63.4	60.4
VAN-B [22]	26.6	INP	53.5	86.8	58.0	47.3	65.5	60.6
		MSFA	55.1 **(+1.6)**	87.7	60.2	48.8	67.3	62.2
Swin-T [41]	28.3	INP	48.4	83.5	50.8	42.8	59.7	55.7
		MSFA	50.2 **(+1.8)**	84.1	53.9	44.1	61.3	58.8
Swin-S [41]	49.6	INP	53.1	87.3	57.8	47.4	63.9	60.6
		MSFA	54.0 **(+0.9)**	87.0	59.2	48.2	64.5	61.9
Swin-B [41]	87.8	INP	53.8	87.8	59.0	49.1	64.6	60.0
		MSFA	55.7 **(+1.9)**	87.8	61.4	50.5	66.5	62.5

A.5 Experimental Results

A.5.1 Main results on SARDet-100K.

The detailed experimental outcomes are presented in Table S7, Table S8, and Table S9, where comprehensive, fine-grained testing metrics are provided. These include AP@50, AP@75, AP@small (AP@s), AP@medium (AP@m), and AP@large (AP@l), offering deeper insights and robust results for model evaluation.

Table S7 serves as an extension of Table 3 from the main paper, showcasing a comparison of various filter-augmented inputs utilizing Faster R-CNN with ResNet-50 as the detection model.

Table S8 expands upon Figure 6(a) of the main paper, and Table S9 expands upon Figure 6(b). These tables centre on the experiments that explore the generalizability of the MSFA framework across different detection frameworks and backbones. Notably, a significant enhancement in performance is observed across various frameworks, including single-stage, two-stage, and query-based frameworks, as well as across a spectrum of backbone architectures, ranging from ResNets and modern-designed ConvNets to Vision Attention Networks (VANs) and Vision Transformer (ViT)-based Swin networks. These results offer compelling evidence of the efficacy and broad applicability of the method we propose.

Table S10: Dataset statistics comparison between DOTA and DIOR. *: multi-scale preprocessed.

Dataset	Images	Instances	Categories	Image Size	Avg. Instance Area
DOTA*	68,324	1,058,641	15	1024*1024	5,021
DIOR	23,463	192,518	20	800*800	12,726

Table S11: Comparison of MSFA and Finetuning Performance under similar computational budgets. INP: Backbones are pretrained on ImageNet.

Model	INP	MSFA Epoch	Finetune Epochs	Total Epochs	Total Iterations	mAP
Faster-RCNN [53]	✓	12	24	36	16.1k	54.5
Faster-RCNN [53]	✓	0	36	36	17.7k	52.8

To ensure a fair comparison, we evaluate MSFA and vanilla detection models under similar computational budgets. In Table S11, we train Faster-RCNN models (with a ResNet-50 ImageNet-1K pretrained backbone) with 12 epochs of MSFA pretraining on the DOTA dataset, followed by finetuning on the SARDet-100K dataset. This is compared to directly finetuning the model for 36 epochs on the SARDet-100K dataset. With the same total number of training epochs and a slightly less total number of iterations, the proposed MSFA achieves a significantly higher (1.7% higher) mAP result on the SARDet-100K test set. MSFA pretraining incorporates general knowledge from both natural and remote sensing datasets, which allows efficient and effective finetuning and helps mitigate overfitting in downstream tasks. It is also important to note that, MSFA pretraining is a one-time effort. The pretrained MSFA models can be reused for finetuning different SAR detection datasets.

A.5.2 Comparison of SARDet-100K with other datasets.

To assess the quality of the proposed SARDet-100K dataset as a large-scale SAR object detection benchmark, we evaluate different models on this dataset and compare the results with those obtained from other popular benchmark datasets, such as SSDD [84] and HRSID [71]. The results are presented in Fig S9. These results indicate that the performance of modern models on our dataset has not yet reached saturation. Among the various models reviewed, there is an 8.4% performance gap between the weakest and strongest models, whereas, for SSDD and HRSID, this gap is only 4.1% and 4.3%, respectively. This suggests that SSDD and HRSID are relatively simple for most existing models, leading to performance saturation on these smaller datasets.

Furthermore, we observed that on these smaller datasets, models with a relatively large number of parameters tend to suffer from performance degradation due to overfitting. For example, ResNet-152 underperforms compared to ResNet-101 on SSDD, and ResNet-101 underperforms compared to ResNet-50 and ResNet-18 on HRSID. However, on the large-scale SARDet-100K, this issue does not arise. On our larger dataset, models continue to benefit from increased model size, indicating that our proposed dataset is suitable for developing relatively larger models for large-scale SAR object detection.

https://doi.org/10.52202/079017-4079

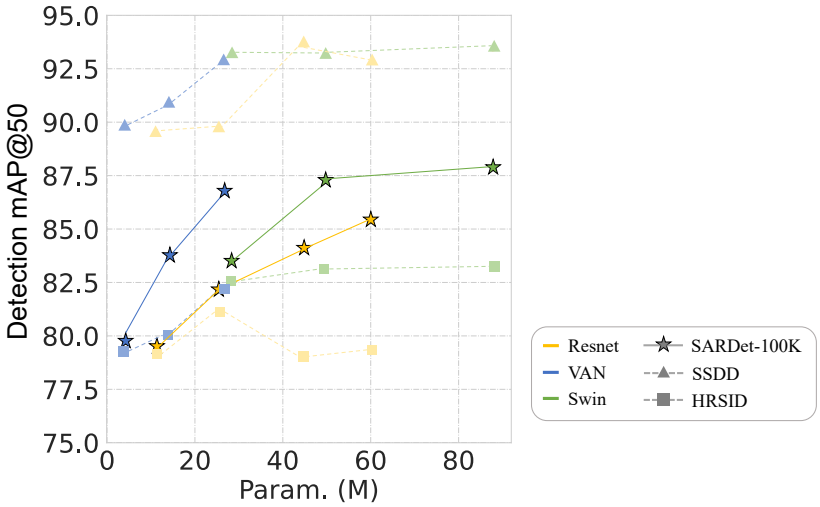

Figure S9: Evaluate different backbone models on SARDet-100K dataset and other previous popular benchmarks (SSDD [84] and HRSID [71]). Backbones are plugged under Faster-RCNN [53] detection framework.

A.6 Implementaion Details

For the ImageNet pretrain, we adopt a 100-epoch backbone pretraining strategy on the Imagenet-1K, with their default training strategy in MMPretrain [11] configurations.

For the second stage of the proposed multistage pretrain, we select the large-scale optical remote sensing DOTA dataset as the main dataset. We also do comparison experiments on the DIOR dataset to find out the downstream performance affection factors on the second stage pretrain dataset. Their detailed information is illustrated in Table S10.

For the DOTA dataset, we perform an extra dataset preprocess because DOTA dataset images have a large range of different image resolutions. The original image contains only 1,411 training images. To have more image and multiscale instances for effective training, we follow [31] to adopt a multi-scale dataset splitting strategy by rescaling the original high-resolution images into three distinct scales (x0.5, x1.0, x1.5), and then cropping each scaled image into 1024×1024 patches with an overlap of each patch of 500 pixels, to avoid destruction division on the instance at patch borders. With the preprocessed dataset, load resize as 1024*1024, with a RandomFlip probability of 0.5. For the DIOR dataset, we train the model by resizing the images as 800*800, with a RandomFlip probability of 0.5.

For finetuning on SARDet-100k, SSDD and HRSID, we train by resizing the image into 800*800, with a RandomFlip probability of 0.5. We train the model by 12 epochs on the train set and test the model on the test set with the 12th epoch checkpoint.

We primarily conduct our experiments using the MMPretrain [11] and the MMDetection [8] frameworks, on 8 RTX-3090 GPUs (24G). For detailed information on the hyperparameters and training settings, please refer to Table S12.

A.7 Detection Result Visualizations

The detection visualization results, comparing the MSFA framework with the traditional ImageNet pretraining approach, are presented in Fig. S10. These results demonstrate that MSFA outperforms the conventional ImageNet backbone pretrain in terms of reducing missed detections, false detection, and improving localization accuracy.

Table S12: Hyper-parameter of pretrain and finetune settings. Cls.: Classification, Det.: Detection, B.S.: Batch Size, L.R.: Learning Rate.

Task / Model	Dataset	Optim.	B.S.	L.R	Epochs
Cls. Pretrain	ImageNet	AdamW	512	1e-8	100
Det. Pretrain	DOTA	AdamW	16	1e-4	12
Det. Pretrain	DIOR	AdamW	16	1e-4	12
Det. Finetune	SARDet-100k	AdamW	16	1e-4	12
Det. Finetune	SSDD	AdamW	32	2.5e-4	12
Det. Finetune	HRSID	AdamW	32	2.5e-4	12
DETR	DOTA/SARDet-100k	AdamW	16	1e-4	150
Deformable-DETR	DOTA/SARDet-100k	AdamW	16	2e-4	50
Dab-DETR	DOTA/SARDet-100k	AdamW	16	1e-4	50
Sparse-RCNN	DOTA/SARDet-100k	AdamW	16	2.5e-5	12

Table S13: ConvNext-B MSFA

Category	mAP	@50	@75	@s	@m	@l
ship	0.669	0.923	0.783	0.653	0.714	0.555
aircraft	0.455	0.753	0.466	0.419	0.458	0.47
car	0.655	0.985	0.792	0.553	0.674	n/a
tank	0.454	0.766	0.427	0.429	0.891	n/a
bridge	0.441	0.885	0.368	0.411	0.609	0.714
harbor	0.711	0.979	0.858	0.601	0.751	0.756
Average	0.564	0.882	0.616	0.511	0.733	0.624

A.8 Failure Scenarios

However, the current model is not without its drawbacks and imperfections. Fig. S11 highlights several failure scenarios. When the input SAR images lack identifiable details or contextual information, it can lead to incorrect classifications. When SAR images contain small and densely packed objects, the model may fail to detect some of them. Poor image quality characterized by fading, blurriness, or overall low resolution, further exacerbates the risk of missed detections. In challenging cases, the detector may also struggle with accurate localization.

Regarding fine-grained category detection performance, Table S13 presents the detection results of Faster-RCNN [53] with ConvNext-B [42] and MSFA pretraining. Notably, the model exhibits relatively low performance for objects with:

- Small sizes, such as Tank (with an average area of 461 pixels)
- Large length-width ratios, such as Bridge
- High appearance variability, such as Airplane

However, the primary focus of this work is to address the domain and model gaps existing in SAR object detection pretraining and finetuning. Our method demonstrates excellent compatibility with most existing deep networks and can seamlessly integrate with models specifically designed to tackle the above challenging scenarios.

https://doi.org/10.52202/079017-4079

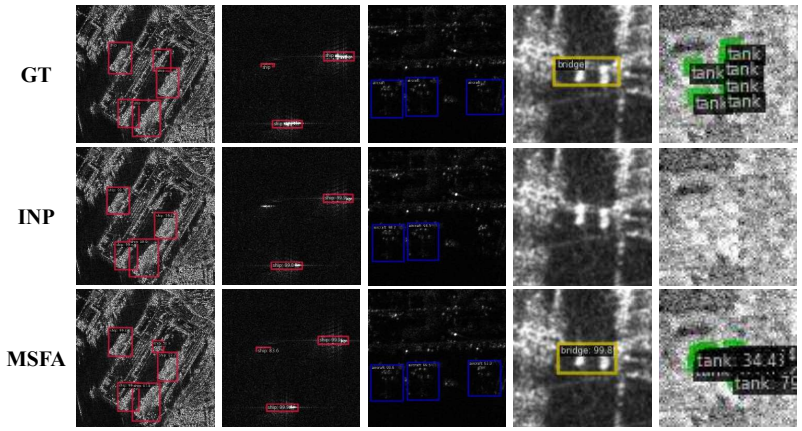

(a) Missing detection

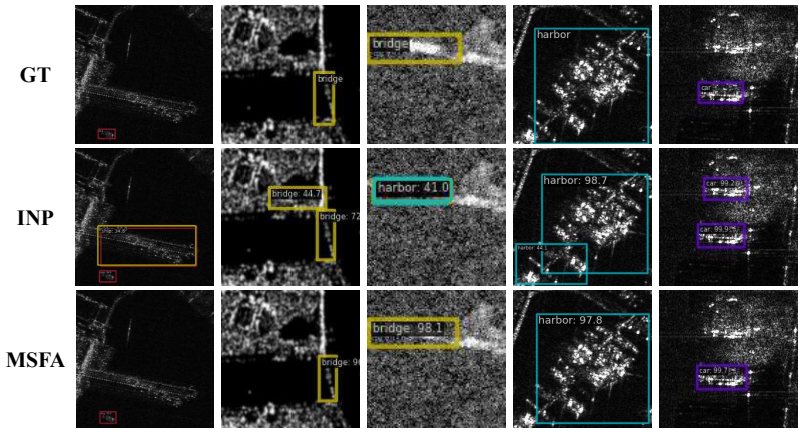

(b) False detection

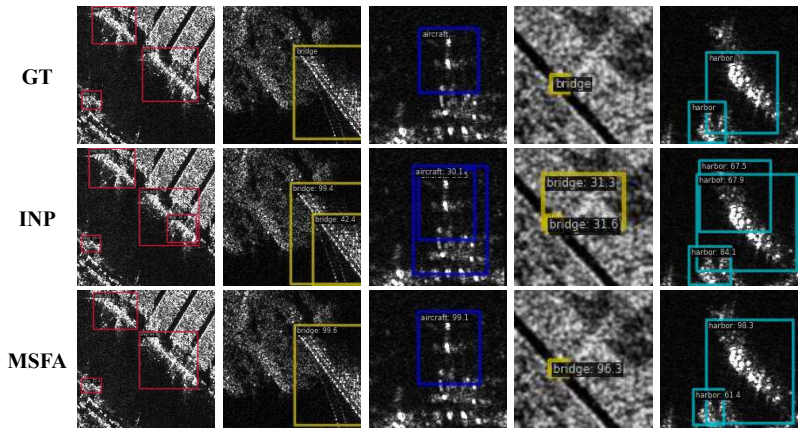

(c) Inaccurate localization

Figure S10: MSFA better than traditional ImageNet backbone pretrain in (a) missing detection, (b) false detection and (c) inaccurate localization

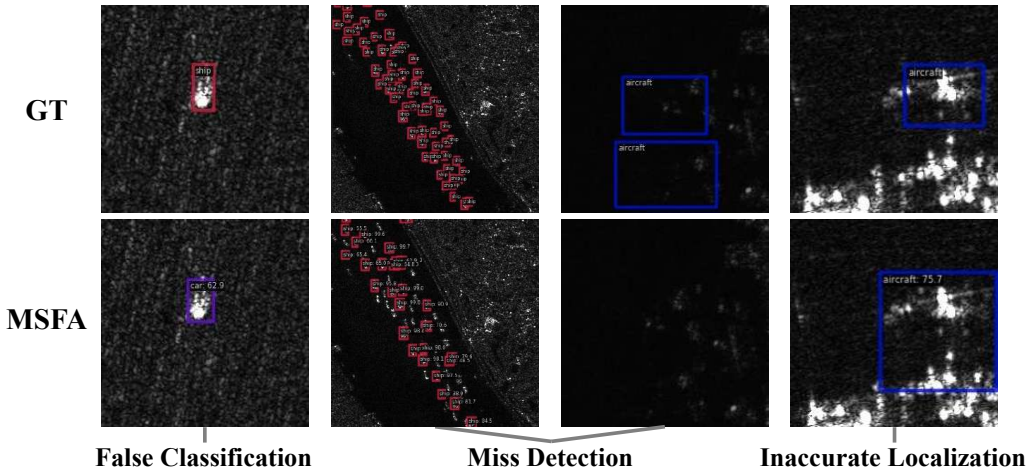

Figure S11: Visulization of failure cases: false classification, miss detection, inaccurate localization.

https://doi.org/10.52202/079017-4079

NeurIPS Paper Checklist

1. **Claims**

   Question: Do the main claims made in the abstract and introduction accurately reflect the paper's contributions and scope?

   Answer: [Yes]

   Justification: The proposed dataset is well explained in Section 3, A.1, A.2, and the proposed pretrain method is elaborated in Section 4. Experiments in Section 5, A.5, A.7 support our claims.

   Guidelines:

   - The answer NA means that the abstract and introduction do not include the claims made in the paper.
   - The abstract and/or introduction should clearly state the claims made, including the contributions made in the paper and important assumptions and limitations. A No or NA answer to this question will not be perceived well by the reviewers.
   - The claims made should match theoretical and experimental results, and reflect how much the results can be expected to generalize to other settings.
   - It is fine to include aspirational goals as motivation as long as it is clear that these goals are not attained by the paper.

2. **Limitations**

   Question: Does the paper discuss the limitations of the work performed by the authors?

   Answer: [Yes]

   Justification: Limitations are discussed in Section 6 and A.8.

   Guidelines:

   - The answer NA means that the paper has no limitation while the answer No means that the paper has limitations, but those are not discussed in the paper.
   - The authors are encouraged to create a separate "Limitations" section in their paper.
   - The paper should point out any strong assumptions and how robust the results are to violations of these assumptions (e.g., independence assumptions, noiseless settings, model well-specification, asymptotic approximations only holding locally). The authors should reflect on how these assumptions might be violated in practice and what the implications would be.
   - The authors should reflect on the scope of the claims made, e.g., if the approach was only tested on a few datasets or with a few runs. In general, empirical results often depend on implicit assumptions, which should be articulated.
   - The authors should reflect on the factors that influence the performance of the approach. For example, a facial recognition algorithm may perform poorly when image resolution is low or images are taken in low lighting. Or a speech-to-text system might not be used reliably to provide closed captions for online lectures because it fails to handle technical jargon.
   - The authors should discuss the computational efficiency of the proposed algorithms and how they scale with dataset size.
   - If applicable, the authors should discuss possible limitations of their approach to address problems of privacy and fairness.
   - While the authors might fear that complete honesty about limitations might be used by reviewers as grounds for rejection, a worse outcome might be that reviewers discover limitations that aren't acknowledged in the paper. The authors should use their best judgment and recognize that individual actions in favor of transparency play an important role in developing norms that preserve the integrity of the community. Reviewers will be specifically instructed to not penalize honesty concerning limitations.

3. **Theory Assumptions and Proofs**

   Question: For each theoretical result, does the paper provide the full set of assumptions and a complete (and correct) proof?

Answer: [NA]

Justification: The paper does not include theoretical results.

Guidelines:

- The answer NA means that the paper does not include theoretical results.
- All the theorems, formulas, and proofs in the paper should be numbered and cross-referenced.
- All assumptions should be clearly stated or referenced in the statement of any theorems.
- The proofs can either appear in the main paper or the supplemental material, but if they appear in the supplemental material, the authors are encouraged to provide a short proof sketch to provide intuition.
- Inversely, any informal proof provided in the core of the paper should be complemented by formal proofs provided in appendix or supplemental material.
- Theorems and Lemmas that the proof relies upon should be properly referenced.

4. **Experimental Result Reproducibility**

   Question: Does the paper fully disclose all the information needed to reproduce the main experimental results of the paper to the extent that it affects the main claims and/or conclusions of the paper (regardless of whether the code and data are provided or not)?

   Answer: [Yes]

   Justification: We give the implementation details in Section A.6. We upload the source code as supplementary material.

   Guidelines:

   - The answer NA means that the paper does not include experiments.
   - If the paper includes experiments, a No answer to this question will not be perceived well by the reviewers: Making the paper reproducible is important, regardless of whether the code and data are provided or not.
   - If the contribution is a dataset and/or model, the authors should describe the steps taken to make their results reproducible or verifiable.
   - Depending on the contribution, reproducibility can be accomplished in various ways. For example, if the contribution is a novel architecture, describing the architecture fully might suffice, or if the contribution is a specific model and empirical evaluation, it may be necessary to either make it possible for others to replicate the model with the same dataset, or provide access to the model. In general. releasing code and data is often one good way to accomplish this, but reproducibility can also be provided via detailed instructions for how to replicate the results, access to a hosted model (e.g., in the case of a large language model), releasing of a model checkpoint, or other means that are appropriate to the research performed.
   - While NeurIPS does not require releasing code, the conference does require all submissions to provide some reasonable avenue for reproducibility, which may depend on the nature of the contribution. For example
     (a) If the contribution is primarily a new algorithm, the paper should make it clear how to reproduce that algorithm.
     (b) If the contribution is primarily a new model architecture, the paper should describe the architecture clearly and fully.
     (c) If the contribution is a new model (e.g., a large language model), then there should either be a way to access this model for reproducing the results or a way to reproduce the model (e.g., with an open-source dataset or instructions for how to construct the dataset).
     (d) We recognize that reproducibility may be tricky in some cases, in which case authors are welcome to describe the particular way they provide for reproducibility. In the case of closed-source models, it may be that access to the model is limited in some way (e.g., to registered users), but it should be possible for other researchers to have some path to reproducing or verifying the results.

5. **Open access to data and code**

https://doi.org/10.52202/079017-4079

Question: Does the paper provide open access to the data and code, with sufficient instructions to faithfully reproduce the main experimental results, as described in supplemental material?

Answer: [Yes]

Justification: We upload the source code as supplementary material. We will release our code and dataset after paper acceptance.

Guidelines:

- The answer NA means that paper does not include experiments requiring code.
- Please see the NeurIPS code and data submission guidelines (`https://nips.cc/public/guides/CodeSubmissionPolicy`) for more details.
- While we encourage the release of code and data, we understand that this might not be possible, so "No" is an acceptable answer. Papers cannot be rejected simply for not including code, unless this is central to the contribution (e.g., for a new open-source benchmark).
- The instructions should contain the exact command and environment needed to run to reproduce the results. See the NeurIPS code and data submission guidelines (`https://nips.cc/public/guides/CodeSubmissionPolicy`) for more details.
- The authors should provide instructions on data access and preparation, including how to access the raw data, preprocessed data, intermediate data, and generated data, etc.
- The authors should provide scripts to reproduce all experimental results for the new proposed method and baselines. If only a subset of experiments are reproducible, they should state which ones are omitted from the script and why.
- At submission time, to preserve anonymity, the authors should release anonymized versions (if applicable).
- Providing as much information as possible in supplemental material (appended to the paper) is recommended, but including URLs to data and code is permitted.

6. **Experimental Setting/Details**

   Question: Does the paper specify all the training and test details (e.g., data splits, hyperparameters, how they were chosen, type of optimizer, etc.) necessary to understand the results?

   Answer: [Yes]

   Justification: We give the implementation details in Section A.6. We also provide training/testing configs in the uploaded code.

   Guidelines:

   - The answer NA means that the paper does not include experiments.
   - The experimental setting should be presented in the core of the paper to a level of detail that is necessary to appreciate the results and make sense of them.
   - The full details can be provided either with the code, in appendix, or as supplemental material.

7. **Experiment Statistical Significance**

   Question: Does the paper report error bars suitably and correctly defined or other appropriate information about the statistical significance of the experiments?

   Answer: [No]

   Justification: Based on our empirical experiments, the reproductive results of the same model are highly consistent. There are significant differences in results between different models, which exceed the margin of error bars. Additionally, we lack sufficient computational resources to calculate error bars for every experiment.

   Guidelines:

   - The answer NA means that the paper does not include experiments.
   - The authors should answer "Yes" if the results are accompanied by error bars, confidence intervals, or statistical significance tests, at least for the experiments that support the main claims of the paper.

- The factors of variability that the error bars are capturing should be clearly stated (for example, train/test split, initialization, random drawing of some parameter, or overall run with given experimental conditions).
- The method for calculating the error bars should be explained (closed form formula, call to a library function, bootstrap, etc.)
- The assumptions made should be given (e.g., Normally distributed errors).
- It should be clear whether the error bar is the standard deviation or the standard error of the mean.
- It is OK to report 1-sigma error bars, but one should state it. The authors should preferably report a 2-sigma error bar than state that they have a 96% CI, if the hypothesis of Normality of errors is not verified.
- For asymmetric distributions, the authors should be careful not to show in tables or figures symmetric error bars that would yield results that are out of range (e.g. negative error rates).
- If error bars are reported in tables or plots, The authors should explain in the text how they were calculated and reference the corresponding figures or tables in the text.

8. **Experiments Compute Resources**

   Question: For each experiment, does the paper provide sufficient information on the computer resources (type of compute workers, memory, time of execution) needed to reproduce the experiments?

   Answer: [Yes]

   Justification: Rough information is given in Section A.6. More details about training time, memory required etc. for each experiment are provided as log files in our source code.

   Guidelines:

   - The answer NA means that the paper does not include experiments.
   - The paper should indicate the type of compute workers CPU or GPU, internal cluster, or cloud provider, including relevant memory and storage.
   - The paper should provide the amount of compute required for each of the individual experimental runs as well as estimate the total compute.
   - The paper should disclose whether the full research project required more compute than the experiments reported in the paper (e.g., preliminary or failed experiments that didn't make it into the paper).

9. **Code Of Ethics**

   Question: Does the research conducted in the paper conform, in every respect, with the NeurIPS Code of Ethics `https://neurips.cc/public/EthicsGuidelines`?

   Answer: [Yes]

   Justification: The research conducted in the paper conforms, in every respect, with the NeurIPS Code of Ethics

   Guidelines:

   - The answer NA means that the authors have not reviewed the NeurIPS Code of Ethics.
   - If the authors answer No, they should explain the special circumstances that require a deviation from the Code of Ethics.
   - The authors should make sure to preserve anonymity (e.g., if there is a special consideration due to laws or regulations in their jurisdiction).

10. **Broader Impacts**

    Question: Does the paper discuss both potential positive societal impacts and negative societal impacts of the work performed?

    Answer: [NA]

    Justification: No societal impact of the work performed.

    Guidelines:

    - The answer NA means that there is no societal impact of the work performed.

https://doi.org/10.52202/079017-4079

- If the authors answer NA or No, they should explain why their work has no societal impact or why the paper does not address societal impact.
- Examples of negative societal impacts include potential malicious or unintended uses (e.g., disinformation, generating fake profiles, surveillance), fairness considerations (e.g., deployment of technologies that could make decisions that unfairly impact specific groups), privacy considerations, and security considerations.
- The conference expects that many papers will be foundational research and not tied to particular applications, let alone deployments. However, if there is a direct path to any negative applications, the authors should point it out. For example, it is legitimate to point out that an improvement in the quality of generative models could be used to generate deepfakes for disinformation. On the other hand, it is not needed to point out that a generic algorithm for optimizing neural networks could enable people to train models that generate Deepfakes faster.
- The authors should consider possible harms that could arise when the technology is being used as intended and functioning correctly, harms that could arise when the technology is being used as intended but gives incorrect results, and harms following from (intentional or unintentional) misuse of the technology.
- If there are negative societal impacts, the authors could also discuss possible mitigation strategies (e.g., gated release of models, providing defenses in addition to attacks, mechanisms for monitoring misuse, mechanisms to monitor how a system learns from feedback over time, improving the efficiency and accessibility of ML).

11. **Safeguards**

    Question: Does the paper describe safeguards that have been put in place for responsible release of data or models that have a high risk for misuse (e.g., pretrained language models, image generators, or scraped datasets)?

    Answer: [NA]

    Justification: The paper poses no such risks.

    Guidelines:

    - The answer NA means that the paper poses no such risks.
    - Released models that have a high risk for misuse or dual-use should be released with necessary safeguards to allow for controlled use of the model, for example by requiring that users adhere to usage guidelines or restrictions to access the model or implementing safety filters.
    - Datasets that have been scraped from the Internet could pose safety risks. The authors should describe how they avoided releasing unsafe images.
    - We recognize that providing effective safeguards is challenging, and many papers do not require this, but we encourage authors to take this into account and make a best faith effort.

12. **Licenses for existing assets**

    Question: Are the creators or original owners of assets (e.g., code, data, models), used in the paper, properly credited and are the license and terms of use explicitly mentioned and properly respected?

    Answer: [Yes]

    Justification: Licenses of merged datasets are put into Table S6. We cited relevant assets, and our proposed dataset collection gets permission from the original dataset owners.

    - The answer NA means that the paper does not use existing assets.
    - The authors should cite the original paper that produced the code package or dataset.
    - The authors should state which version of the asset is used and, if possible, include a URL.
    - The name of the license (e.g., CC-BY 4.0) should be included for each asset.
    - For scraped data from a particular source (e.g., website), the copyright and terms of service of that source should be provided.

- If assets are released, the license, copyright information, and terms of use in the package should be provided. For popular datasets, `paperswithcode.com/datasets` has curated licenses for some datasets. Their licensing guide can help determine the license of a dataset.
- For existing datasets that are re-packaged, both the original license and the license of the derived asset (if it has changed) should be provided.
- If this information is not available online, the authors are encouraged to reach out to the asset's creators.

13. **New Assets**

    Question: Are new assets introduced in the paper well documented and is the documentation provided alongside the assets?

    Answer: [Yes]

    Justification: We provided detailed information about the proposed dataset and detailed documentation about our source code.

    Guidelines:

    - The answer NA means that the paper does not release new assets.
    - Researchers should communicate the details of the dataset/code/model as part of their submissions via structured templates. This includes details about training, license, limitations, etc.
    - The paper should discuss whether and how consent was obtained from people whose asset is used.
    - At submission time, remember to anonymize your assets (if applicable). You can either create an anonymized URL or include an anonymized zip file.

14. **Crowdsourcing and Research with Human Subjects**

    Question: For crowdsourcing experiments and research with human subjects, does the paper include the full text of instructions given to participants and screenshots, if applicable, as well as details about compensation (if any)?

    Answer: [NA]

    Justification: The paper does not involve crowdsourcing nor research with human subjects.

    Guidelines:

    - The answer NA means that the paper does not involve crowdsourcing nor research with human subjects.
    - Including this information in the supplemental material is fine, but if the main contribution of the paper involves human subjects, then as much detail as possible should be included in the main paper.
    - According to the NeurIPS Code of Ethics, workers involved in data collection, curation, or other labor should be paid at least the minimum wage in the country of the data collector.

15. **Institutional Review Board (IRB) Approvals or Equivalent for Research with Human Subjects**

    Question: Does the paper describe potential risks incurred by study participants, whether such risks were disclosed to the subjects, and whether Institutional Review Board (IRB) approvals (or an equivalent approval/review based on the requirements of your country or institution) were obtained?

    Answer: [NA]

    Justification: The paper does not involve crowdsourcing nor research with human subjects.

    Guidelines:

    - The answer NA means that the paper does not involve crowdsourcing nor research with human subjects.
    - Depending on the country in which research is conducted, IRB approval (or equivalent) may be required for any human subjects research. If you obtained IRB approval, you should clearly state this in the paper.

https://doi.org/10.52202/079017-4079

- We recognize that the procedures for this may vary significantly between institutions and locations, and we expect authors to adhere to the NeurIPS Code of Ethics and the guidelines for their institution.
- For initial submissions, do not include any information that would break anonymity (if applicable), such as the institution conducting the review.